Nocturnal Evolution of Cloud Clusters over Eastern China during the Intensive Observation Periods of GAME/HUBEX in 1998 and 1999

Zhuxiao LI

Graduate School of Environmental Earth Science, Hokkaido University, Sapporo, Japan

Takao TAKEDA, Kazuhisa TSUBOKI

Hydrospheric Atmospheric Research Center, Nagoya University, Nagoya, Japan

Kuranoshin KATO

Faculty of Education, Okayama University, Okayama, Japan

Masayuki KAWASHIMA

Institute of Low Temperature Science, Hokkaido University, Sapporo, Japan

and

Yasushi FUJIYOSHI

Institute of Low Temperature Science, Hokkaido University, Sapporo, Japan
Frontier Research Center for Global Change, Japan Agency for Marine-Earth Science and Technology, Yokohama, Japan

(Manuscript received 9 August 2004, in final form 16 October 2006)

Abstract

Global Water Cycle Experiment (GEWEX)–Asian Monsoon Experiment (GAME)/Huaihe River Basin Energy Water Cycle Experiments (GAME/HUBEX) were conducted during the Meiyu period in 1998 and 1999. Using infrared brightness temperature (T_{BB}) data of the Geostationary Meteorological Satellite (GMS)-5, we investigated the diurnal variation of 61 long-lasting cloud clusters that developed during GAME/HUBEX Intensive Observation Periods (IOPs). More than two-thirds of the cloud clusters, named nocturnal-type clusters, attained a convective peak between midnight and early morning, with most peaking between 00 and 02 LST. Almost all of these nocturnal-type cloud clusters developed in, or south of the Meiyu frontal zone. The other clusters, named evening-type cloud clusters, peaked from late afternoon to evening, and were less intense than the nocturnal clusters.

Corresponding author: Yasushi Fujiyoshi, Institute of Low Temperature Science, Hokkaido University, Sapporo 060-0819, Japan.
E-mail: fujiyo@lowtem.hokudai.ac.jp

GAME-Reanalysis (Version 1.5) data showed that the ageostrophic wind component over a large domain to the south of the Meiyu front shifted from easterly to southerly, and increased the velocity of the southwesterly airflow largely at low levels at nighttime (02 LST). This southwesterly ageostrophic synoptic-scale low-level jet (S-LLJ) transported large amounts of water vapor to the Meiyu front, forcing large moisture convergence within, and immediately south of the Meiyu frontal zone. The low-level moisture convergence, and the S-LLJ itself are proposed to support the nocturnal evolution or redevelopment of cloud clusters.

1. Introduction

Cloud clusters are a type of mesoscale convective complex (MCC) composed of deep convective clouds, with an organized and multi-scale structure. In wide regions from the Equator to midlatitudes, MCCs are primary contributors to annual precipitation and have a profound influence on terrestrial energy and water cycles (e.g., Maddox 1980; Wetzel et al. 1983; Leary and Rappaport 1987; Ohsawa et al. 2001).

Past studies have shown clear diurnal variations in cloud clusters over tropical oceans. Gray and Jacobson (1977) found that significant early morning heavy rainfall was closely associated with very deep convection in organized cloud systems. They suggested that the diurnal cycle is forced by differences in upper-level radiative cooling (heating) between cloudy and clear regions at night (in the daytime), respectively. Randall et al. (1991) examined radiative cooling from high clouds (e.g., cirrus and anvil clouds). Both daytime heating, and nighttime cooling, occurred in the upper troposphere where high clouds existed. The largest instability drove convection at night. Diurnal variations in the amount of water vapor also influence the diurnal cycle of convection (e.g., Sui et al. 1997; Kubota and Nitta 2001). Moisture increased in the boundary layer during the evening, and boundary-layer clouds appeared around 20 LST. Radiative cooling near the top of the boundary-layer cloud destabilizes the lower atmosphere, and transports moisture to the free atmosphere from the boundary layer. Shallow convection can then develop into deep convection.

Many studies have examined diurnal variations in cloud clusters over the United States. Anderson and Arritt (1998) studied large, long-lasting convective systems over the United States. They found preferred nocturnal development in both MCCs and persistent elongated convective systems. Maddox (1983) and Cotton et al. (1983) found that nocturnal MCCs occur in convectively unstable environments that are characterized by strong horizontal convergence, associated with a low-level jet (LLJ) in the vicinity of a quasi-stationary frontal zone. The diurnal variation of the LLJ plays a fundamental role in the nocturnal development of MCCs (Trier and Parsons 1993). Nocturnal MCC development is favored in regions north of a quasi-stationary frontal zone, because high-θe air transported northward by the LLJ into a region of significantly colder mid-tropospheric conditions causes particularly high convective available potential energy (CAPE). Resultant adiabatic mesoscale ascent is particularly strong near the northern terminus of the LLJ. This ascent causes significant cooling above the jet axis. Cooling associated with the ascent, and the continuous strong moisture advection, reduces convective inhibition so that air parcels can more easily reach the level of free convection (LFC).

Some past studies have investigated diurnal variations in convective activity and heavy rainfall. Misumi (1999) used radar echo composites over Japan from the warm seasons of 1988 to 1993 to study diurnal variations in precipitation from different cloud categories. Cumulus-scale precipitation clouds, forced by boundary-layer heating, showed a dominant afternoon peak. Other large-scale precipitation clouds, with scales of hundreds of kilometers showed a diurnal cycle with a morning peak, regardless of any land–sea circulation. Asai et al. (1998) investigated diurnal variations of convection, indicated by cloudiness over eastern China and the western Pacific. They found a diurnal variation in cloudiness that resulted from the superposition of large diurnal cycles, and smaller

semidiurnal variations. The semidiurnal cycle over land had two peaks, 03–05 LST (LST = GMT + 8) and 15–17 LST, with similar amplitudes. A diurnally varying maximum in cloudiness appeared near dusk over the Tibetan Plateau, and at midnight over the Sichuan Basin. The latter was attributed to both locally induced convection, and eastward movement of cloud clusters that originated over the Tibetan Plateau.

Organized meso-α-, or meso-β-scale deep convective cloud systems frequently develop and propagate in the Meiyu frontal zone in Eastern Asia (Ninomiya et al. 1988a, b). The cloud clusters cause heavy rainfall, with maximum rates of a few hundred millimeters per day (Chen 1983; Ding 1992), and flash or persistent floods along the Meiyu front over China (Tao et al. 1980), Korea, and southern Japan. Case studies to examine mesoscale cloud clusters associated with the Meiyu front began in the 1970s (e.g., Matsumoto et al. 1970; Ninomiya and Akiyama 1971, 1974). The horizontal scale of the cloud clusters was usually several-hundred kilometers, and had a multi-scale structure: meso-β and meso-γ convective systems were embedded within the clusters (Akiyama 1984a, b; Ninomiya et al. 1988a, b). Intense rainfalls of 50–100 mm hr^{-1} were present under the highest cloud shields, where infrared brightness temperature (T_{BB}) was colder than $-70°C$ (Ninomiya et al. 1981). Chen et al. (1998a, b) simulated the evolution of a typical convective rainstorm (cloud cluster) along the Meiyu front that caused heavy rainfall over the Jianghuai plain, and showed that a large latent heat release is vital to rainstorm development. Latent heat release aided the development of a mesolow at low levels within the cloud cluster. Warm and moist air parcels accelerated toward the low, creating a southwesterly mesoscale low-level jet (m-LLJ). Further strengthening of the innermost strong vertical motion, low-level convergence, and upper level divergence associated with the cloud cluster would also be attributable to latent heat release.

Several researchers have studied a series of typical meso-α-scale cloud clusters that developed over China and propagated to Japan and the Pacific, from 12 to 15 July 1979 (Ninomiya and Tatsumi 1981; Akiyama 1984a, b; Ninomiya et al. 1981, 1988a, b). The cloud clusters on 12–15 July 1979 showed clear diurnal evolution, developing in the early morning (03–09 LST) and weakening in the early afternoon (~15 LST) (Akiyama 1984a). Kato et al. (1995) examined the diurnal variation of cumulonimbus clusters that developed between June and August 1979 over eastern China (110°E–120°E). They found that the clusters appeared frequently in the Meiyu frontal zone over central China, both in the day and at night during the Meiyu period. In contrast, clusters appeared mostly during the evening over both north and northeast China during the Meiyu period, and central China during midsummer. The dominant peak in the evening was attributed to maximum ground surface temperatures in the afternoon.

However, no past research has concentrated on the diurnal variations in convection peaks associated with mesoscale cloud clusters that develop over eastern China. Therefore, this study was designed to clarify whether an obvious diurnal variation exists in convection associated with cloud clusters over eastern China, and, if diurnal variation exists, to identify the forcing mechanism. Such information on diurnal variation will help explain the mechanisms of cloud cluster development and the interactions between cloud clusters and the environment.

The Global Water Cycle Experiment (GEWEX)–Asian Monsoon Experiment (GAME) monitored the role of the Asian monsoon in the global energy and water cycle, to improve the simulation and seasonal prediction of the Asian monsoon and regional water resources. The Huaihe River Basin Energy Water Cycle Experiments (HUBEX) project, one of four GAME subprojects, was conducted during Meiyu periods in 1998 and 1999. Ding et al. (2001) and Fujiyoshi et al. (2006) have provided details of the main observations, including surface observations, radiosonde soundings, multi-Doppler radar observations, hydrological observations, and land surface flux measurements. Many scales of cloud system appeared in the Meiyu frontal zone (e.g., Ding and Liu 2000) during the intensive observation period (IOP), when the Meiyu front was very active and long lasting, between June and August 1998. Because large floods occurred over eastern China several times during this period and abun-

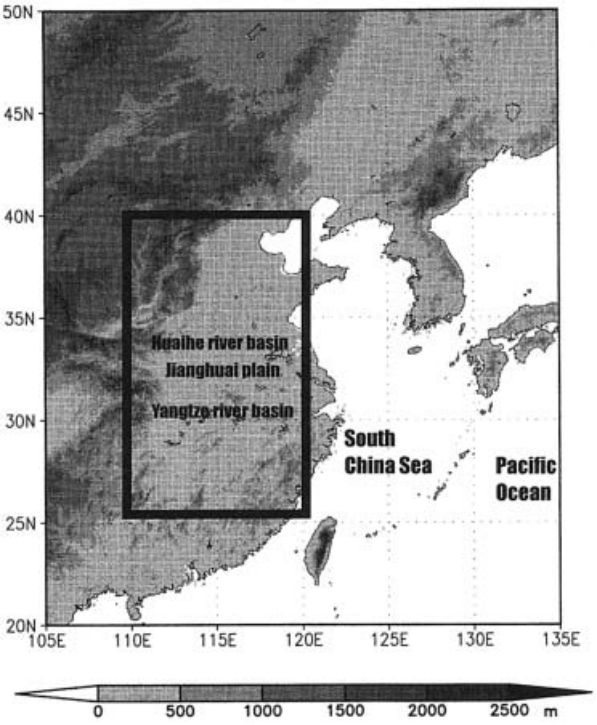

Fig. 1. Map of Eastern Asia with topography. Solid black lines outline the analysis domain over eastern China from 110–120°E and 25–40°N. Topographic contours are shown at 500-m intervals.

dant data are available from the IOP, these months were chosen as the main period of analysis.

This paper is laid out in the following manner. Section 2 outlines the data and methods. Section 3 describes the diurnal-cycle characteristics of cloud clusters that developed in August of 1998. Section 4 examines the diurnal variation in the low-level horizontal wind field (including the synoptic LLJ) over eastern China, especially over the southern part of the domain. Section 5 outlines diurnal variations in low-level water vapor flux and moisture convergence over the Meiyu frontal convergence zone. Section 6 explores diurnal variations in wind and the resultant moisture convergence field during other periods of 1998. Finally, Sections 7 and 8 contain a discussion and summary, respectively.

2. Data and methods of analysis

Figure 1 shows the analysis domain that extends from 110°E to 120°E and from 25°N to 40°N and includes the Yangtze river basin, Jianghuai plain and Huaihe river basin. Severe floods sometimes occur within these basins when cloud clusters repeatedly recur. The evolution of each cloud cluster was studied using hourly T_{BB} data from Geostationary Meteorological Satellite (GMS) infrared (IR) imagery for 1998 (June, July, and August), and 1999 (June and July). The grid size of the data was 20 km in 1998, and 10 km in 1999. Any influence of the change in grid size between 1998 and 1999 can be ignored because the horizontal scale of the cloud clusters exceeded 100 km, and because the coarse T_{BB} distribution and T_{BB} area rather than the fine details of the structure were the focus of this study.

Since our main concern is the evolution of a long-lasting meso-β-scale cloud cluster, we added two criteria (1 and 2) in addition to those (3 and 4) given by Takeda and Iwasaki (1987). (1) The lifetime (from develop to decay) of the cloud cluster is longer than 12 hours. (2) Maximum cloud area exceeds 6×10^4 km^2, and maximum cloud diameter exceeds 250 km. (3) The oval-shaped cloud mass region of T_{BB} lower than -50°C is larger than 100 km in diameter, and (4) the horizontal gradient of T_{BB} is large near the rim of the cloud mass (at least for a part of the rim). Regions with T_{BB} colder than

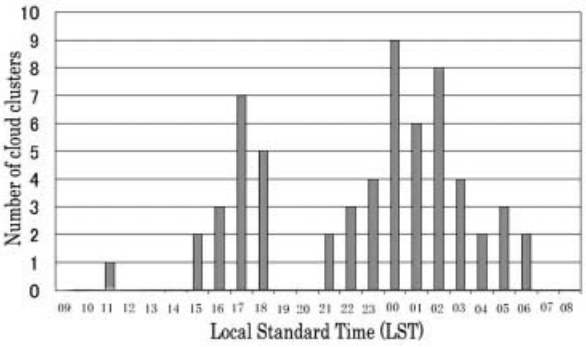

Fig. 2. Diurnal cycle of the occurrence frequency of the dominant convective peak for the 61 analyzed cloud clusters in June, July, and August 1998, and June and July 1999. Local Standard Time (LST) is Beijing Standard Time.

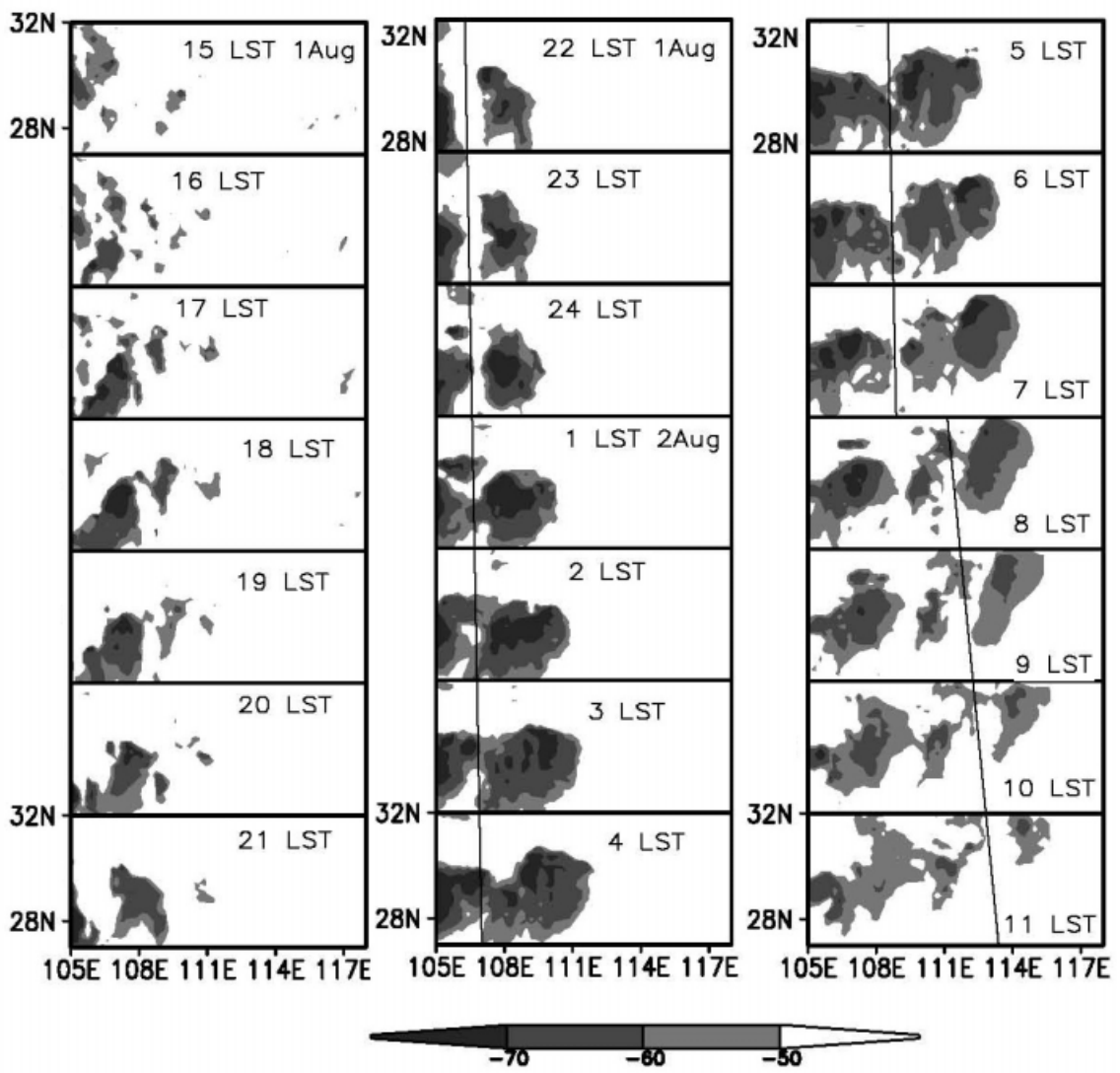

Fig. 3. Hourly time series of low T_{BB} distribution for a typical nocturnal-type cloud cluster that persisted from 15 LST 1 August to 11 LST 2 August 1998. The analyzed cloud cluster is at the right side of the solid line in every panel.

−70°C relate directly to heavy rainfall (Ninomiya et al. 1981; Mapes and Houze 1993). Iwasaki and Takeda (1993) referred to such cold T_{BB} areas as "cold regions". The regions correspond to meso-β-scale convective systems within the meso-α-scale cloud cluster (Ninomiya et al. 1988a).

Every cloud cluster that satisfied the above definitions was traced manually in hourly time series of T_{BB} images. Special upper-air soundings were taken within the meso-α scale domain of GAME/HUBEX, but the experiment area was not sufficiently large to allow study of the evolution of cloud clusters, and diagnosis of the surrounding environmental conditions. Therefore, this study used GAME-Reanalysis (Ver. 1.5) data provided by the Japan Meteorological Agency (JMA) to study the atmospheric conditions surrounding the developing cloud clusters. This data set covers a large horizontal scale (several thousand kilometers) and can resolve cloud cluster trajectories throughout their life stages. The reanalysis data set has a spatial resolution of 0.5×0.5 degrees in longitude

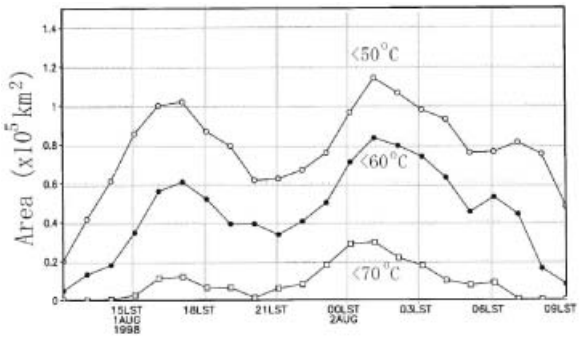

Fig. 4. Hourly time series of the low T_{BB} area within the cloud cluster shown in Fig. 3. Thresholds of T_{BB} for the low T_{BB} areas are -50°C (open circles), -60°C (solid circles), and -70°C (open squares), respectively. The Y-axis denotes the low T_{BB} area with units of 10^5 km^2.

and latitude, and time resolution of 6 hours. All data (z, u, v, temperature, mixing ratio) were interpolated onto 17 levels (1000, 925, 850, 700, 600, 500, 400, 300 ... 50 hPa), except for specific humidity data, which were interpolated only to levels at or below 300 hPa.

3. Diurnal cycle of cloud clusters

There were 61 deep, long-lasting cloud clusters satisfying the selection criteria during the study period. Figure 2 shows the diurnal cycle in the peak time of the 61 cloud clusters; the peak time was defined as the hour when the cold region in the cluster was largest. Analyzed cloud clusters were divided into two types based on the dominant peak time. Nocturnal-type cloud clusters, 43 of the 61 clusters, peaked between early evening and early morning (between 20 and 06 LST); more than half of these nocturnal peaks (23/43) occurred between 00 and 02 LST. The remaining cloud clusters (17 of 61) peaked between afternoon and early evening (from 15 to 18 LST), and were classified as evening-type. One cloud cluster peaked at 11 LST and did not belong to either type.

Figure 3 exemplifies the evolution of a typical nocturnal-type cloud cluster as indicated by the time series of the distribution of T_{BB}. This cloud cluster developed around 16 LST on 1 August 1998 and decayed into shallow clouds at 11 LST on 2 August. The first convective peak occurred around 18 LST. Convection subsequently weakened, and the cold region disappeared around 21 LST. However, the area of the cold regions increased dramatically after 22 LST, and then peaked again at 02 LST. The area of the cold region at 02 LST was much larger than that at 18 LST. The cloud cluster slowly decayed after 02 LST, splitting into two smaller parts with warmer T_{BB} around 08 LST. Figure 4 shows time series of areas with T_{BB} colder than -50, -60, and -70°C within this cloud cluster. The time series show a dominant peak in very early morning, and a secondary peak in the evening. Convection was stronger in the early morning than in the evening; the area of the cold region in the early morning (1.5×10^4 km^2) was 2.5 times larger than that in the evening (0.6×10^4 km^2).

Nocturnal-type cloud clusters had different characteristics from evening-type clusters as summarized in Table 1. Nocturnal- and evening-type clusters typically peaked at around 02 LST and 17 LST, respectively. Mean life spans for nocturnal-type and evening-type clusters were 19 and 14 hours, respectively. The mean peak areas of the high cloud shield (defined as $T_{BB} < -50$°C) for the two types were nearly equivalent, i.e., 11.4×10^4 km^2 for the nocturnal type, and 10.9×10^4 km^2 for the evening type. However, the mean peak area of the cold region was much larger for nocturnal-

Table 1. Characteristics of nocturnal- and evening-type cloud clusters as indicated by mean values of various indexes.

Type of cloud cluster	Number of cloud cluster	Life time (hour)	Peak time (LST)		Peak area ($\times 10^4$ km^2)	
			Cold region	High cloud shield	Cold region	High cloud shield
Nocturnal type	43	19	02	04	3.3	11.4
Evening type	17	14	17	17	2.1	10.9

Table 2. Peak position of analyzed cloud clusters relative to the Meiyu front.

Position of the geometrical center of the peak area of the cold region relative to the Meiyu front	Number of cloud clusters	
	Nocturnal type	Evening type
100–200 km south of the Meiyu front	26	7
Within the domain from 100 km south to 50 km north of the Meiyu front (over the Meiyu front)	13	3
Far from the frontal zone (north or south)	4	7

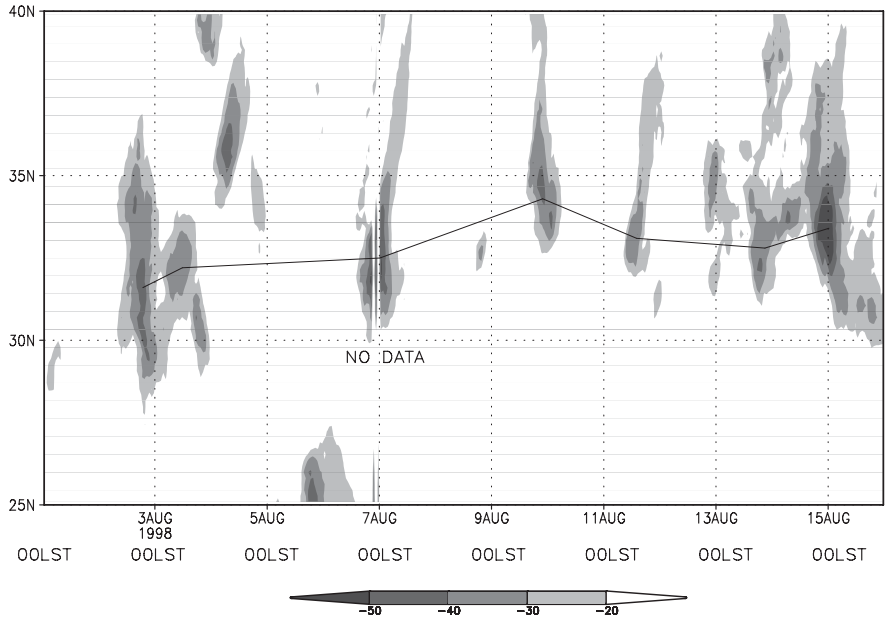

Fig. 5. Time–latitude cross-sections of low T_{BB} (°C) averaged from 110 to 120°E for 1–15 August 1998.

type clusters (3.3×10^4 km^2) than for evening-type clusters (2.1×10^4 km^2), indicating that convection was more intense in nocturnal-type clusters than in evening-type clusters. The cold region in nocturnal-type clusters was largest around 02 LST, two hours before the peak of the high cloud shield. In evening-type clusters, in contrast, the two areas peaked nearly simultaneously. The later peak in the high cloud shield of nocturnal-type clusters might have been caused by anvil cloud expansion near the tropopause after maximum deep convection (Kubota and Nitta 2001). The fundamental reasons for differences in characteristics between nocturnal- and evening-type clusters remain unclear, but are likely related to the different thermodynamic environments and resulting dynamic structure within the two types of cloud cluster.

Nocturnal-type cloud clusters developed just over or immediately south of the Meiyu front. The Meiyu front position can be determined using the latitudinal gradient of equivalent potential temperature (Kato 1985) (for more detail, see Section 4.1). Table 2 summarizes the "peak position" of the analyzed cloud clusters, which is defined by the geometric center of the peak area of the cold region relative to the Meiyu front. Almost all (39/43) nocturnal-type cloud clusters peaked near the Meiyu front. Of those 39 cloud clusters, most (26) peaked due south (100–200 km) of the Meiyu front. The remaining 13 clusters peaked over the Meiyu front; the geometric centers of the clusters

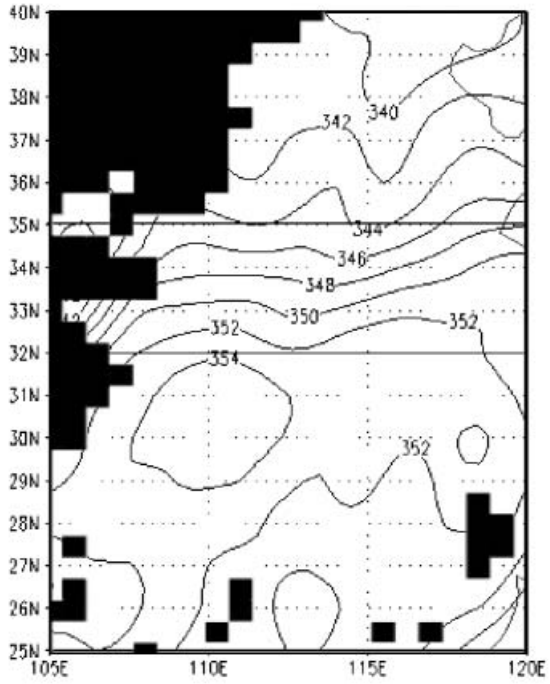

Fig. 6. Horizontal distribution of the equivalent potential temperature (K) at 850 hPa averaged for 1–15 August 1998. The mean equivalent potential temperature is contoured at 2-K intervals. The area between the two solid lines overlaps the large gradient of θ_e, which represents the mean Meiyu frontal zone during that period. Coast line is shown by thick lines.

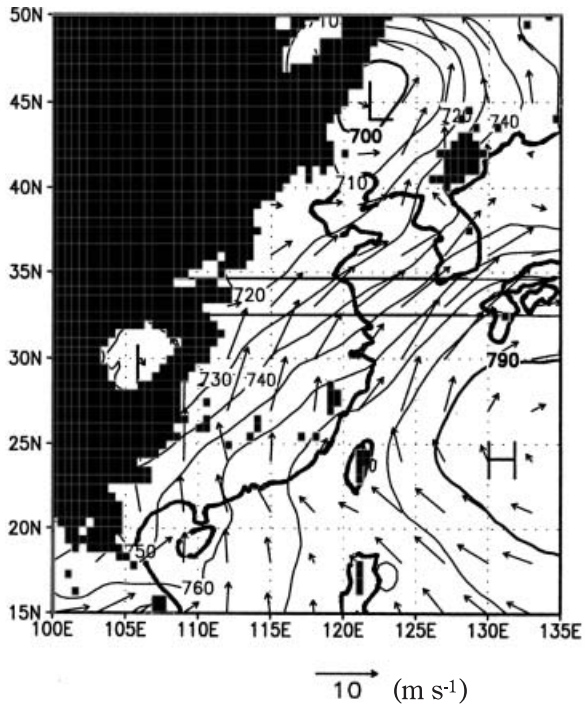

Fig. 7. Geopotential height (contours, in m) and horizontal wind (vectors, in m s^{-1}) fields over Eastern China at 925 hPa averaged for 1–15 August 1998. The isohypse contour interval is 10 m. The area between the two solid lines indicates the mean Meiyu frontal zone in Fig. 6. *H* and *L* denote high and low pressure centers, respectively. Topography is shaded in the figure.

with diameters exceeding 100 km were located within the band-shaped area from 100 km south to 50 km north of the Meiyu front. Only four nocturnal-type cloud clusters peaked far from the Meiyu front. Regions south of, and over the Meiyu front are suggested to be favorable locations for the development of nocturnal-type cloud clusters. Local topography is unlikely to influence the development of nocturnal-type cloud clusters. In contrast, the locations where evening-type cloud clusters peaked showed no clear relationship to distance from the Meiyu front, but were partly related to the local topography.

4. Diurnal variations in wind fields over eastern China from 1–15 August 1998

Maddox (1983), Cotton et al. (1983), and Trier and Parsons (1993) suggested that a nocturnal low-level jet (LLJ), and an east–west oriented front play important roles in the nocturnal development of cloud clusters over central North America. The evolution of clusters is closely linked to a synoptic southwesterly LLJ in the warm sector of the Meiyu front over South China (Ninomiya and Akiyama 1974; Chen 1983; Chen and Yu 1988). Chen (1983) noted that the LLJ transports warm and moist air at low levels; this transport increases convective instability and lowers the level of free convection, subsequently helping to strengthen the convective cloud cluster.

Diurnal variations in low-level wind fields were examined over eastern China, especially near and south of the Meiyu front, using data from 1 to 15 August 1998, a period of frequent nocturnal-type cloud clusters. The Meiyu front

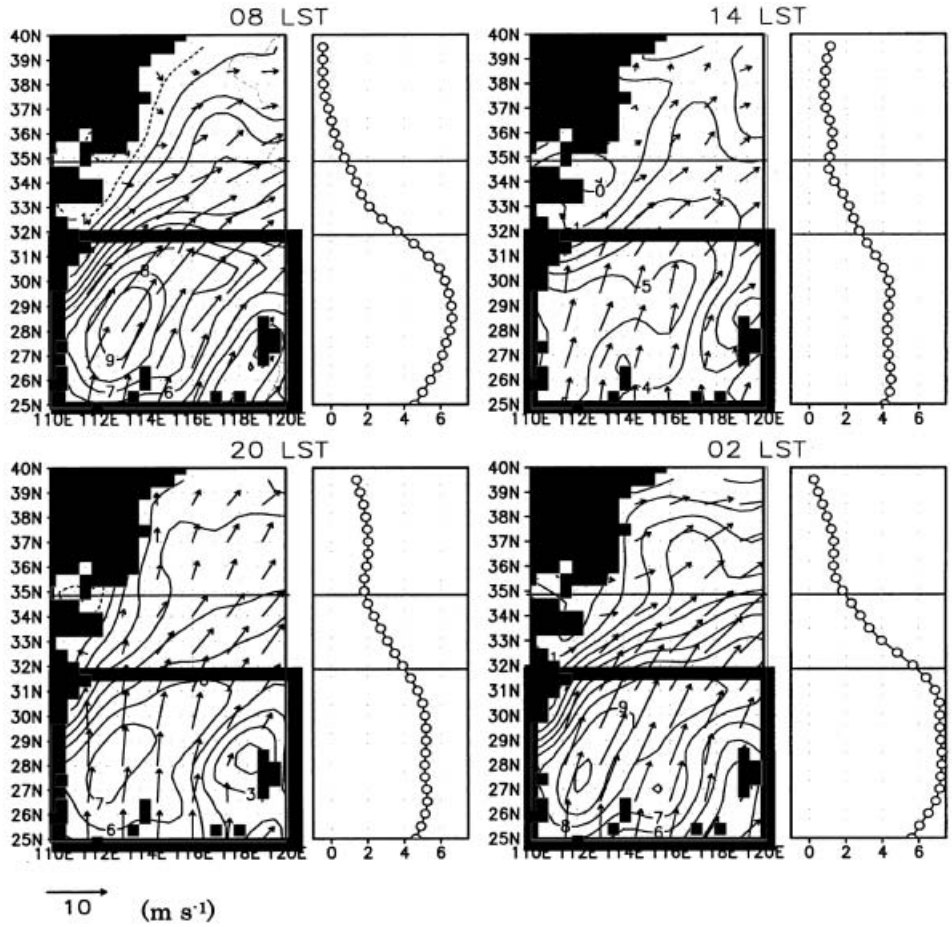

Fig. 8. Diurnal cycles (at 08, 14, 20, and 02 LST) of the mean horizontal wind distribution (left panel at each time) and latitudinal variation of the zonal mean (110–120°E) southerly wind component (right panel at each time) at 925 hPa averaged for 1–15 August 1998. Vectors show the horizontal wind (m s^{-1}); contours indicate the meridional component of horizontal wind (v, m s^{-1}). The two solid lines in each panel bound the area of the mean Meiyu frontal zone (32–35°N) during that period. The domain from 110 to 120°E and from 25 to 32°N surrounded by the black solid rectangle is the South Domain.

was nearly stationary during this period, which simplified study of temporal variability in wind fields.

4.1 The stationary Meiyu front during the selected analysis period

Figure 5 shows the time–latitude cross-section from 1 to 15 August of the cloud area with $T_{BB} < -20$°C averaged from 110°E to 120°E. Synoptic conditions were nearly stationary during this period. Position shift in the geometric center of the area of zonal mean T_{BB} shows that little (less than 200 km) north–south movement of the Meiyu frontal zone occurred. The Meiyu front position can be determined using the latitudinal gradient of equivalent potential temperature (Kato 1985), because the Meiyu front is characterized by latitudinally large humidity contrasts, rather than by temperature contrasts (Akiyama 1973; Ninomiya et al. 1981) over China. Figure 6 shows the mean equivalent potential temperature (θ_e) at 850 hPa. The large gradient of time-averaged θ_e ranged from 32°N to 35°N, indicating that the Meiyu front moved very little during this period. In addition, the largest

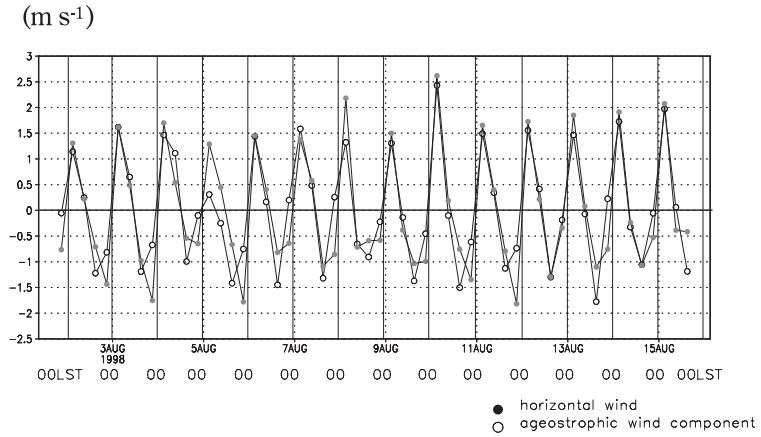

Fig. 9. Six-hourly time series (at 08, 14, 20, and 02 LST) of the temporal deviation of the areal mean meridional component of the horizontal wind (solid circles, m s^{-1}) and of the corresponding ageostrophic wind (open circles, m s^{-1}) over the South Domain at 925 hPa. The deviations of the two variables are the differences from the 5-point time running mean. Solid lines perpendicular to the X-axis denote 00 LST.

monthly precipitation amounts occurred in a narrow band oriented west–east in the region (Ding et al. 2001). The small shift in the Meiyu front suggests that time-averaged meteorological components reflect typical atmospheric conditions for the period.

Figure 7 shows the time–averaged geopotential height and horizontal wind vector fields at 925 hPa. Typical pressure and circulation patterns during the Meiyu season over eastern Asia were present. Two solid lines indicate the Meiyu frontal zone determined by the large gradient of equivalent potential temperature in Fig. 6. The Meiyu frontal zone extended from west to east near the Jianghuai plain. A major depression over northeastern China occurred north of the Meiyu frontal zone. The strong western Pacific subtropical high (WPSH) was located to the southeast of the Meiyu front. A secondary depression, the southwest (SW) vortex, was farther west, around (30°N, 105°E). A significant southwesterly synoptic-scale LLJ (S-LLJ, >10 m s^{-1}) existed between the WPSH and the SW vortex, and extended from the South China Sea to Korea and Kyushu, Japan.

4.2 Diurnal variation in low-level horizontal wind at 925 hPa

Figure 8 shows the diurnal variation in the S-LLJ. The horizontal wind distribution at 925 hPa, averaged for the period of analysis, is shown in the left panel at 08, 14, 20, and 02 LST. The right panel shows the zonal mean (from 110 to 120°E) southerly wind component for these four times. The area within the two solid lines in the left panel is the Meiyu frontal zone. The time-averaged, low-level horizontal winds (left panel) show distinct diurnal variations, especially over the domain south of the Meiyu frontal zone (from 25 to 32°N, and from 110 to 120°E). This area, bounded by a solid rectangle, is henceforth called the South Domain. Low-level wind speeds over the South Domain at 02 LST were much larger than at 14 LST, especially for the southerly wind component, as shown by the contour. The zonal mean southerly wind component in the right panel also reflects time variations in the horizontal wind at 925 hPa.

Diurnal variations in the southerly wind component over the South Domain are more distinct in 6-hourly time series of the area mean within the South Domain (curve with solid circle in Fig. 9). Variables shown are deviations from a 24-hour running mean. Diurnal variations in the southerly wind component over the South Domain clearly occur daily, with a maximum at 02 LST, and a minimum at 14 LST. In contrast, the velocity of the southwesterly wind over the Meiyu frontal zone (left panel at each time in Fig. 8) shows no distinct

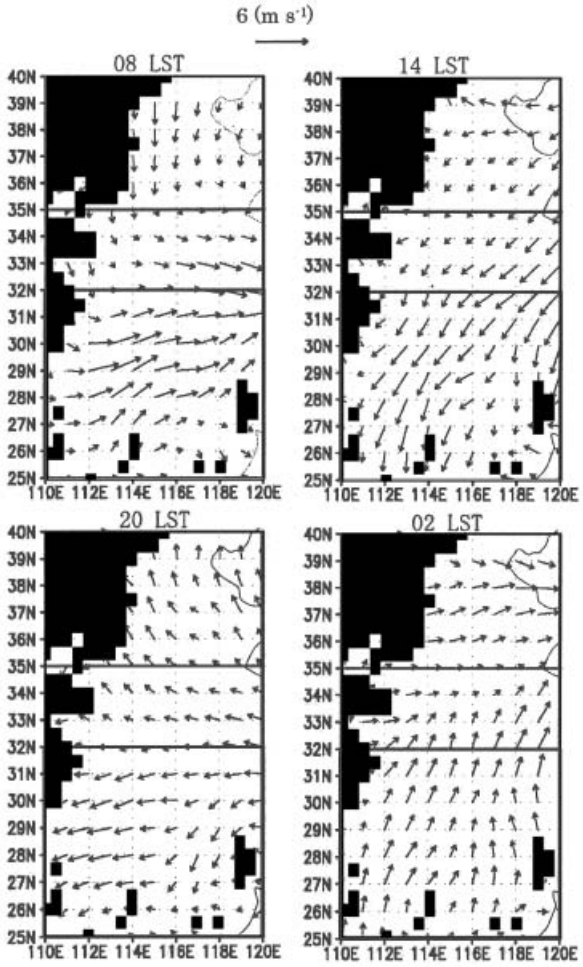

Fig. 10. Diurnal cycle (08, 14, 20, and 02 LST) of horizontal wind deviation ($m\ s^{-1}$) from the daily mean at 925 hPa averaged for 1–15 August 1998. The two solid lines bound the area of the mean Meiyu frontal zone (32–35°N).

diurnal variation, changing little with time. Winds north of the Meiyu front have much smaller velocities and time variability. The latitudinal variation of the zonal mean southerly wind component (the right panel at each time in Fig. 8) clearly shows that the strong southerly wind at 02 and 08 LST over the South Domain weakened dramatically within the Meiyu frontal zone (about 32–35°N). The southerly wind at 14 and 20 LST also decreased with increasing latitude, but over a much smaller range. The sharp latitudinal decrease in the southerly winds near and within the Meiyu frontal zone at 02 LST, reflects moisture convergence over that domain (see next section).

Diurnal variations in the horizontal wind at 925 hPa are more clearly shown in Fig. 10 as deviations at each time from the daily mean. Clockwise wind shifts were apparent over the analysis domain, especially over the South Domain. This finding will be discussed in Section 7.

4.3 *Diurnal variation in low-level ageostrophic and geostrophic winds over the South Domain*

The horizontal wind was decomposed into geostrophic and ageostrophic components to study further the diurnal variation of the low-level horizontal wind. The components were calculated from the following formulae:

$$V_g(\mu_g, v_g) = (-[1/f]\partial\Phi/\partial y, [1/f]\partial\Phi/\partial x)$$

$$V_{ag} = V - V_g$$

In these formulae, V_g is the geostrophic wind, f is the Coriolis parameter, Φ is the geopotential height, V_{ag} is the ageostrophic wind, and V is the horizontal wind. The two components were calculated every 6 hours from the data set.

Figure 11 shows ageostrophic winds at 925 hPa averaged for 1–15 August of 1998 at 08, 14, 20, and 02 LST. The presence of a diurnal cycle is apparent. Ageostrophic winds were easterly, or east–southeasterly, over the South Domain and within the Meiyu frontal zone at 14 and 20 LST. The winds shifted clockwise to southerly and south–southeasterly at 02 LST. The southerly component of the ageostrophic wind at 02 LST is larger than at 14 and 20 LST. A distinct diurnal variation in the southerly component of the ageostrophic wind over the South Domain is very clear in Fig. 9, which shows time series of the area mean meridional component of the ageostrophic wind (lines with open circles). The diurnal variation of the southerly component of the ageostrophic wind is similar to the diurnal variation in the corresponding wind field, with a maximum at 02 LST, and a minimum at 14 LST. Differences between the southerly wind components and the ageostrophic component are very small, indicating that the time variation of the geostrophic wind over the South Domain is also small, as expected. The similarity between the time variation of the southerly wind components

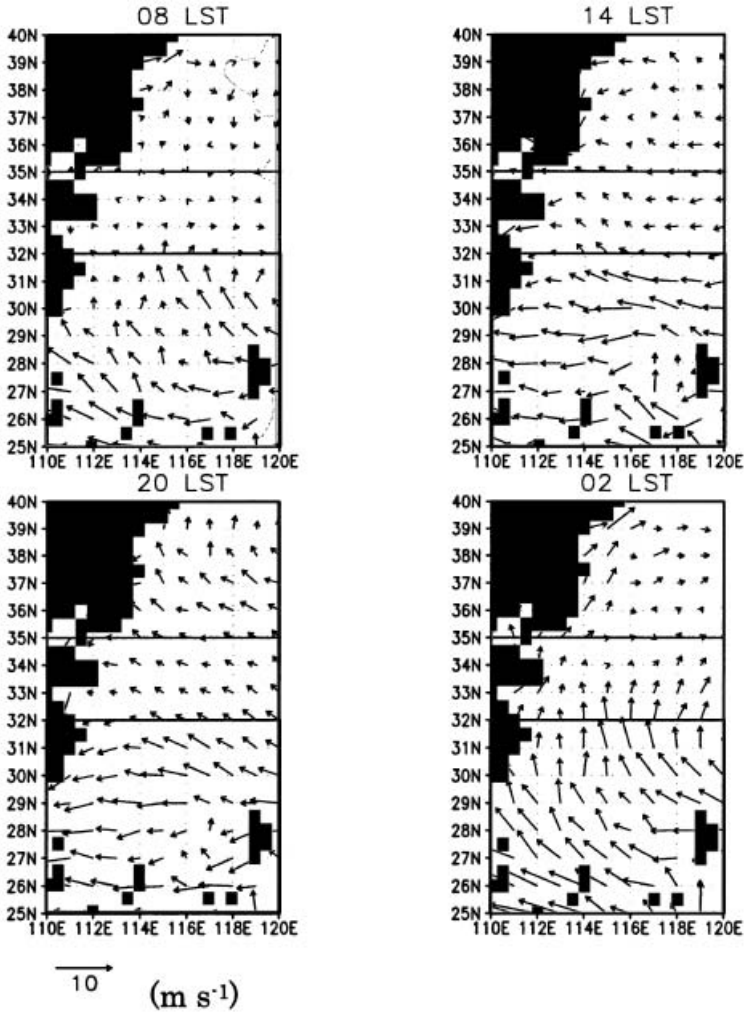

Fig. 11. Diurnal cycle (at 08, 14, 20, and 02 LST) of the ageostrophic wind at 925 hPa averaged for 1–15 August 1998 within the analysis domain. The two solid lines in each panel bound the area of the mean Meiyu frontal zone during this period.

and the time variation of the ageostrophic components suggests that nocturnal intensification of horizontal wind resulted from diurnal variations in the ageostrophic wind.

Figure 12 shows the time difference of averaged geostrophic and ageostrophic wind components between 02 and 14 LST at 925 hPa over eastern China. Time variations in geostrophic wind components (Fig. 12a) were much smaller than variations in the ageostrophic wind component (Fig. 12b). The diurnal variation of the low-level horizontal wind was controlled mainly by the ageostrophic component. As at 925 hPa, a band of strong wind extended from southwest to northeast over eastern China at all levels (not shown). Wind direction shifted slightly with height from south–southwesterly to almost westerly because the western Pacific subtropical high (WPSH) extended into China with height. Horizontal wind fields at 925 and 850 hPa show a significant diurnal variation with a maximum at 02 LST, and a minimum at 14 LST. There was, however, almost no diurnal variation in the horizontal wind fields at and above 700 hPa (not shown). This indicates that the influence of boundary-layer turbulent mixing on the horizontal wind field decreases with height (see discussion in Section 7).

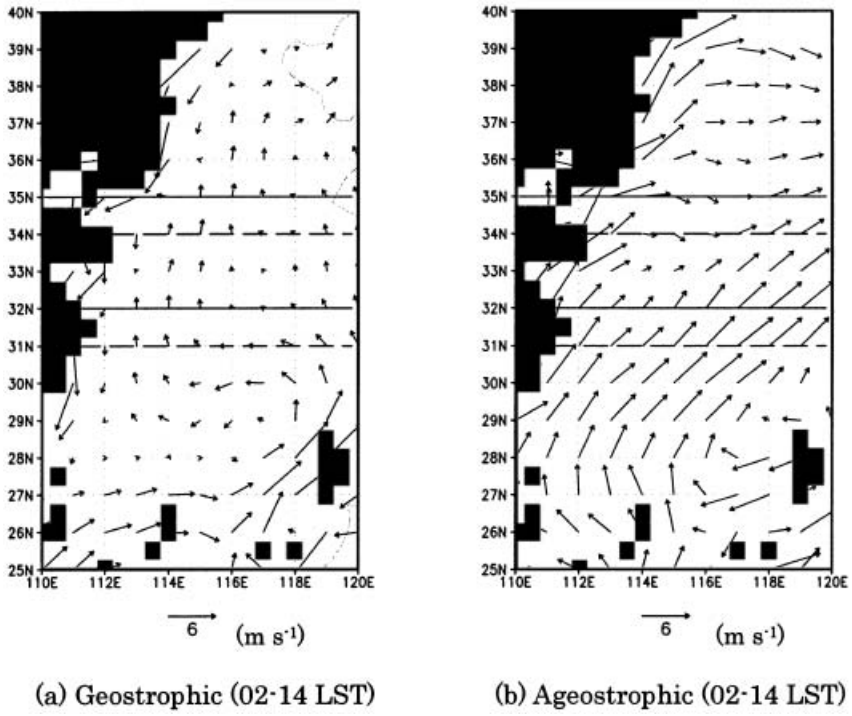

Fig. 12. (a) Time variation of the geostrophic wind component (m s^{-1}) of horizontal wind from 14 to 02 LST (02–14 LST) at 925 hPa averaged for 1–15 August 1998. (b) Same as (a) except for ageostrophic wind component (m s^{-1}). The two solid lines bound the area of the mean Meiyu frontal zone. The two dashed lines surround the area of maximum moisture convergence (31–34°N) (see Fig. 14).

5. Diurnal variations in water vapor flux in the lower troposphere and moisture convergence over the Meiyu frontal convergence zone

Water vapor mixing ratios are generally highest in the lower troposphere and decrease with height. Evaporation from the ground surface and vertical and horizontal advection of water vapor modify the total amount of water vapor in the atmosphere. Water vapor sources include the many paddy fields in the South Domain. Shinoda and Uyeda (2002) suggested that afternoon evaporation from the paddy fields in the Jianghuai plain increases the amount of water vapor in the lower troposphere during the evening.

Figure 13 illustrates the differences in averaged horizontal water vapor flux between 02 and 14 LST at 925 hPa. The average values were computed for 1–15 August 1998 over the analysis domain. South–southwesterly water vapor fluxes over the South Domain were much larger at 02 LST than at 14 LST, especially between 27°N and 32°N, 400–500 km south of the Meiyu front. Stronger southerly and westerly components of water vapor flux are obvious over the South Domain. The amplitude of the difference in the Meiyu frontal zone decreases with latitude from south to north. Large vapor fluxes at 925 hPa over the South Domain at 02 LST, and rapid decreases in flux from south to north within the Meiyu frontal zone forced low-level moisture convergence (see next section) that supported the nocturnal development of cloud clusters. Moisture flux at 850 hPa (not shown) shows clear but smaller diurnal variation compared to flux at 925 hPa.

The large gradient of water vapor flux at 02 LST over and just south of the Meiyu frontal zone in Fig. 13 indicates that nocturnal northward water vapor flux decreased dramatically just south of the Meiyu front. This decreasing of the northward flux from south to north

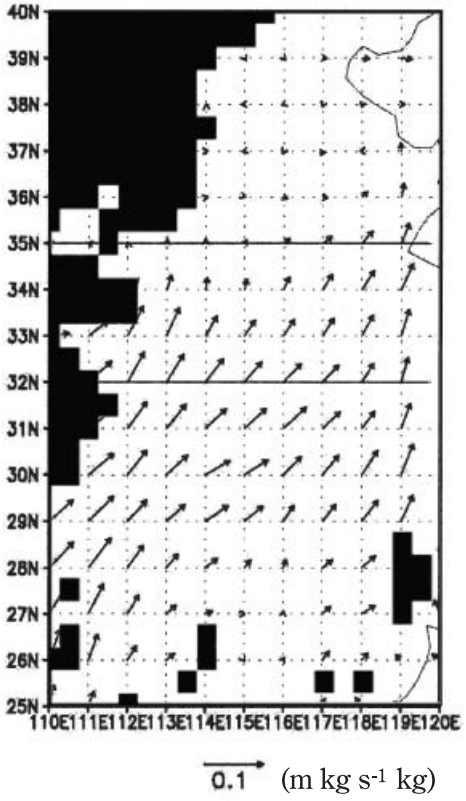

Fig. 13. Differences in horizontal water vapor flux (m·kg s^{-1}·kg) from 14 to 02 LST at 925 hPa over eastern China averaged for 1–15 August 1998. The area within the two solid lines denotes the Meiyu frontal zone.

forced water vapor convergence over the domain at 02 LST. Figure 14 shows the diurnal cycle (at 08, 14, 20, and 02 LST) of the mean horizontal moisture divergence field at 925 hPa, averaged for the analysis period. Strong water vapor convergence at 02 LST exists between 31–34°N and 110–120°E, an area that includes the southern part of the Meiyu frontal zone and areas just to its south, hereafter named the Meiyu frontal convergence zone (MFCZ). Moisture convergence occurred within this region during other times, but the convergence was weaker and only over smaller areas.

There is a larger area of low-level moisture convergence over the MFCZ at 925 hPa than at 850 hPa at night. This change with height is clear in Fig. 15, which shows vertical profiles of area–mean moisture divergence over the MFCZ at 08, 14, 20, and 02 LST. The area–mean moisture convergence (negative moisture divergence) shows a clear diurnal variation, with a significant maximum at 02 LST at 925 hPa. The moisture convergence (1.15×10^{-7} s^{-1}) was almost quadruple that at 14 LST (0.3×10^{-7} s^{-1}), and about twice that at 08 LST. Moisture convergence at 02 LST decreased rapidly with height and showed no diurnal variation, at least above 700 hPa.

Strong low-level moisture convergence over the MFCZ at night possibly enhances the development of cloud clusters and heavy nocturnal rainfall over the MFCZ. Figure 16 shows diurnal variations (02–14 LST) in a convective instability index determined by computing the difference between equivalent potential temperature at 850 and 500 hPa ($\theta_{e500}-\theta_{e850}$) (Akiyama 1984a, b; Kato 1985). Mean values for the analysis period are used. The difference in convective instability is negative over the MFCZ (31–34°N and 110–120°E), indicating an increase in destabilization of the lower atmosphere during the period 14 to 02 LST.

6. Diurnal variations in wind and moisture convergence fields at 925 hPa during other periods of 1998

The low-level wind fields in June and July of 1998 also showed diurnal variation similar to that of August, with an 02 LST maximum and a 14 LST minimum. Figure 17 indicates the time variation in the horizontal wind field at 925 hPa from 08 to 02 LST averaged for 19–30 July 1998. The area within the two solid lines represents the Meiyu frontal zone during that period. The increase in the meridional component of horizontal wind is obvious over the domain south of the Meiyu front at 02 LST compared to 14 LST. Over the northern part of the Meiyu front zone, the diurnal variation in the horizontal wind is not clear. Distinct diurnal variation in the meridional component of horizontal wind over the domain south of the Meiyu front at 925 hPa also occurred in the mean wind field during 15–25 June 1998 (not shown).

Low-level moisture flux in June and July 1998 also showed a diurnal cycle similar to that in August. Figure 18 shows the diurnal variation (at 08, 14, 20, and 02 LST) of moisture convergence at 925 hPa averaged for 19–30 July 1998. As in August, a wide area of strong moisture convergence appeared at 02

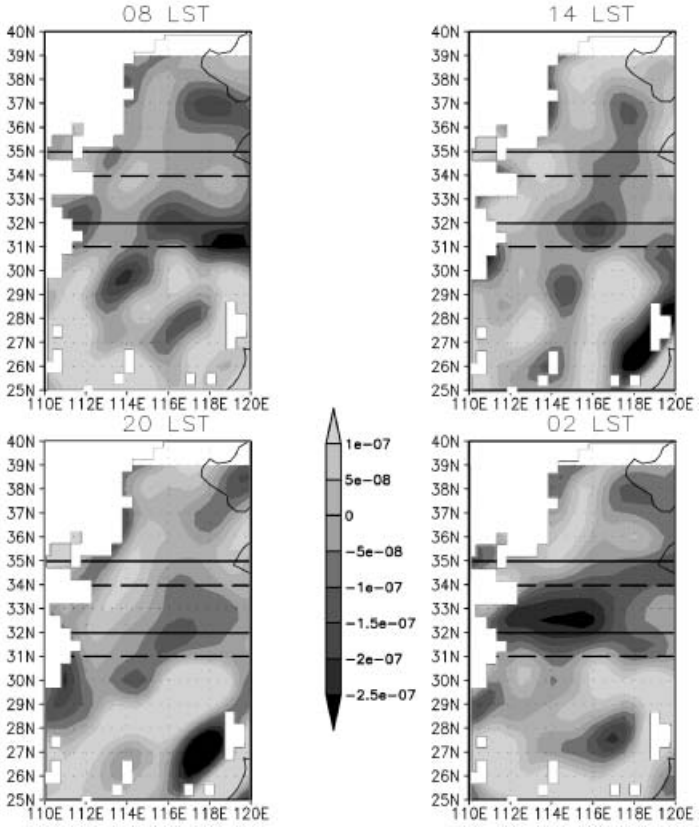

Fig. 14. Diurnal cycle (08, 14, 20, and 02 LST) of the moisture divergence field at 925 hPa averaged for 1–15 August 1998. A negative value of moisture divergence indicates moisture convergence. The two solid lines bound the area of the mean Meiyu frontal zone (32–35°N). The two dashed lines surround the area of maximum moisture convergence (31–34°N) at each time, especially at 02 LST, named the Meiyu Front Convergence Zone (MFCZ).

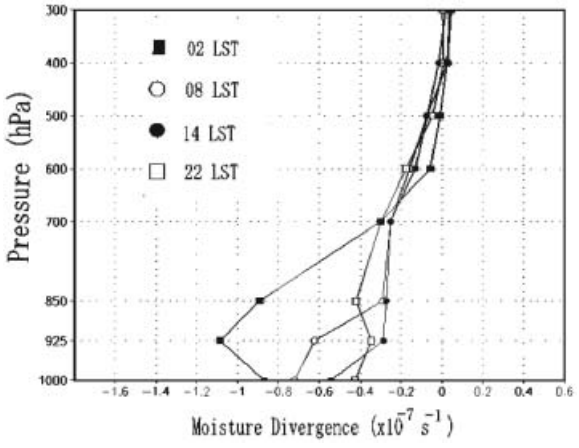

Fig. 15. Vertical profiles of the area mean moisture divergence (10^{-7} s^{-1}) within the MFCZ from 1000 to 300 hPa at 08, 14, 20, and 02 LST, averaged for 1–15 August 1998.

LST within the band-shaped area (27 to 30°N), an area that included the southern part of the Meiyu frontal zone, and areas just to its south. In contrast, very little moisture convergence occurred at this level at 14 and 20 LST.

Figure 19 shows 925-hPa wind and moisture divergence fields at 02 LST on 29 July 1998. A nocturnal-type cloud cluster peaked near the Meiyu front at this time. The trajectory of this cloud cluster, given by its 3-hourly positions, is also shown. The cloud cluster originated near (31.5°N, 111°E) at 17 LST, and its southern boundary rapidly expanded southward. A large area of deep convection developed in the cloud cluster as the southern part of the cluster entered a region where low-level southwesterly winds, and water vapor fluxes were large. This cloud cluster subsequently peaked at 02 LST with a large, very cold T_{BB} area centered near

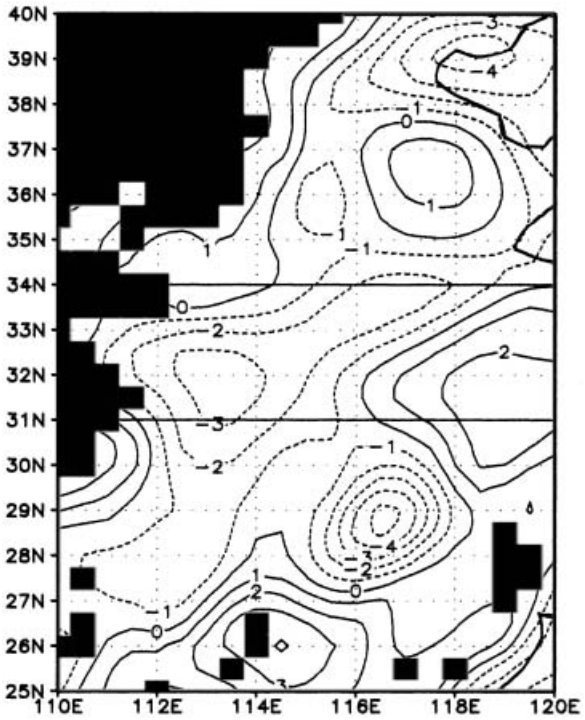

Fig. 16. Differences in the convective instability index ($\theta e_{500}-\theta e_{850}$) from 14 to 02 LST over eastern China averaged between 1 and 15 August 1998. Negative (dashed contour) and positive (solid contour) values indicate increased and decreased destabilization in the lower atmosphere, respectively.

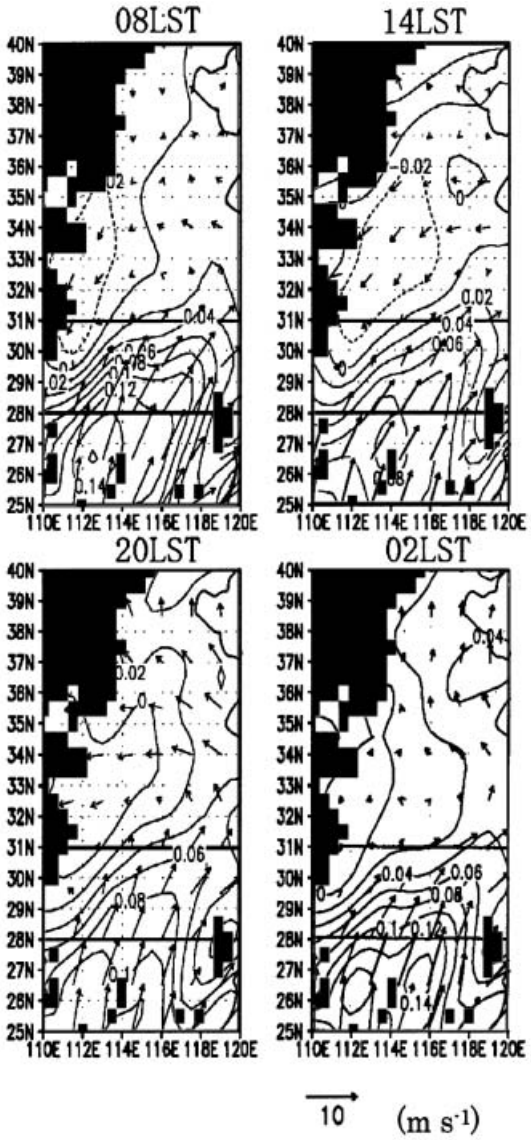

Fig. 17. Time variation of horizontal wind (m s^{-1}) from 08 to 02 LST at 925 hPa over the domain 25°N–40°N and 110°E–120°E. Horizontal winds were averaged for 19–30 July 1998. Vectors show the horizontal wind (m s^{-1}); contours indicate the meridional component of horizontal wind (v, m s^{-1}). As in Fig. 6, the area between the two solid lines overlaps a large gradient of θ_e, which represents the mean Meiyu frontal zone during that period.

(30°N, 114°E). Maximum moisture convergence at 925 hPa was in and south of the area of the cold region. These results indicate that nocturnal low-level moisture convergence is an important factor influencing the development of strong nocturnal convection in cloud clusters.

7. Discussion

The temporal and spatial resolutions of the GAME-Reanalysis dataset are too coarse to study the dynamic processes that affect the development of cloud clusters, or their interaction with the environment. Observations at finer temporal and spatial resolution of wind fields, or other meteorological factors have been limited to much smaller domains than those required to study diurnal variations of cloud clusters. Discussion of the diurnal variation of cloud clusters is limited to possible dynamic pro-

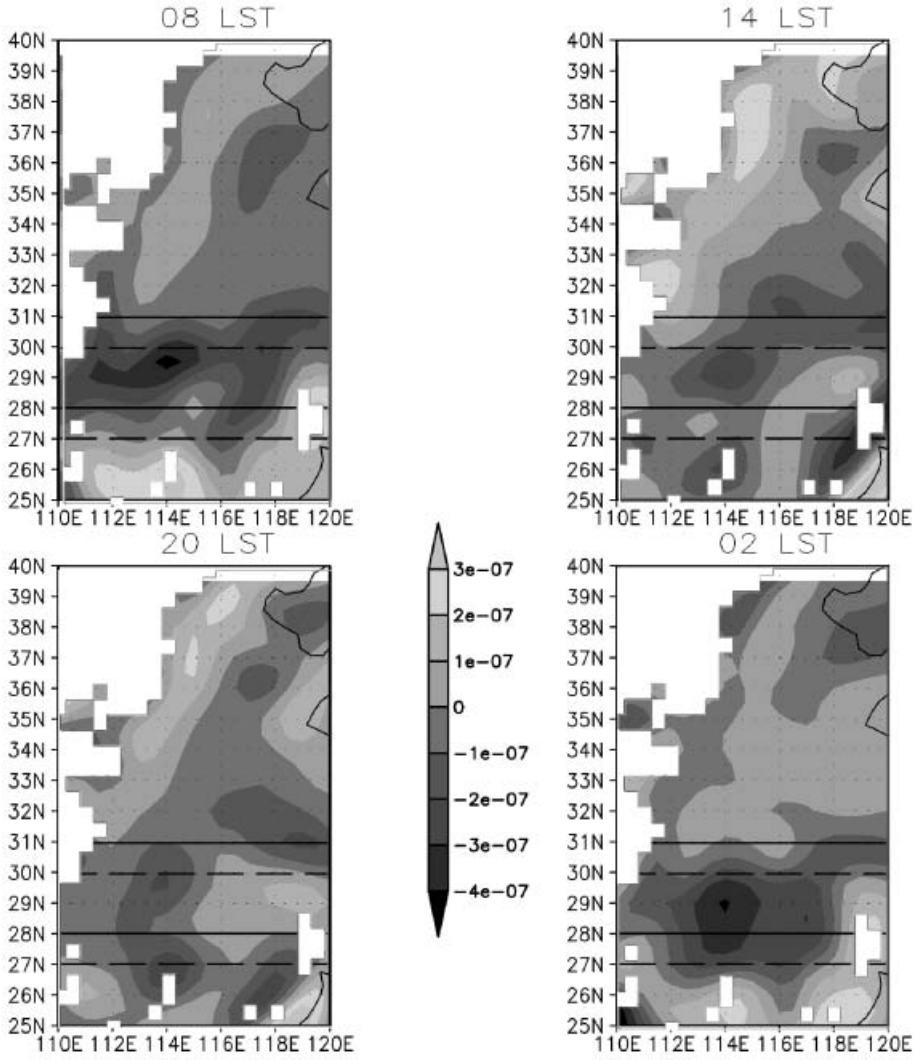

Fig. 18. Diurnal cycle (08, 14, 20, and 02 LST) of moisture divergence (contours, in 10^{-7} s^{-1}) at 925 hPa averaged for 19–30 July 1998. A negative value of moisture divergence indicates moisture convergence. The two solid lines at each panel bound the area of the mean Meiyu frontal zone (28°N–31°N) during that period. The two dashed lines surround the MFCZ (27°N–30°N).

cesses that favor the nocturnal development of cloud clusters over, or south of the Meiyu front. Nocturnal cloud cluster development is likely caused by the enhancement of the southwesterly S-LLJ, and the resulting stronger moisture convergence south of the Meiyu front at night. Therefore, only the reason why the diurnal variation in the low-level wind field is obvious over the South Domain will be discussed below.

Diurnal variations in the low-level horizontal wind over the South Domain are attributed to strong boundary-layer mixing forced by surface solar heating. Figure 20 shows diurnal changes in vertical profiles of the mean potential temperature for 1–15 August 1998 at (28°N, 115°E) (over the South Domain). At 14 and 20 LST, the vertical profile is almost upright, and potential temperature changes little with height, between 1000 and 850 hPa. The boundary layer is well mixed because of strong solar heating at those times. In contrast, profiles of potential temperature show a large slant at 02 and 08 LST, which suggests that only weak mixing was ongoing at those times.

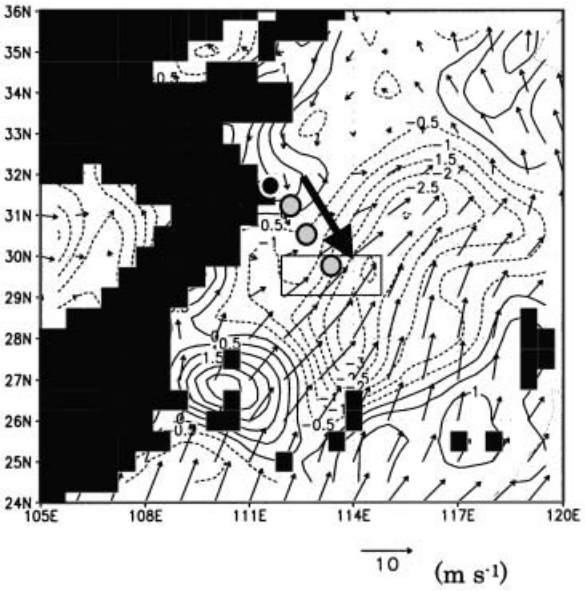

Fig. 19. Horizontal distributions of the wind field (vectors, m s^{-1}) and moisture divergence (contours, 10^{-6} s^{-1}) at 925 hPa at 02 LST on 29 July 1998, when a typical nocturnal-type cloud cluster attained its prominent convection peak. The solid circles indicate the geometric centers of the cloud cluster from 17 LST on 28 July to the peak time at 3-hour intervals. The thick arrow indicates its movement (from northwest to southeast). The small rectangle surrounds the cold region of the cloud cluster at peak time.

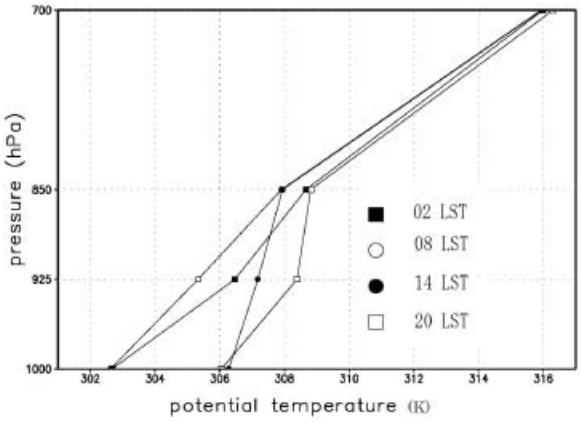

Fig. 20. Diurnal cycle of vertical profiles of potential temperature (K) at (115°E, 27°N) at lower levels (1000–700 hPa) averaged for 1–15 August 1998.

GAME/HUBEX sounding data (for details, see Ding et al. [2001] and Fujiyoshi et al. [2006]), which show more detail because of a finer interval in the vertical, have similar diurnal variations in boundary-layer mixing. Strong surface daytime heating significantly influences boundary-layer winds. Figure 21 shows a longitude–height cross-section of the averaged southerly wind component at 30°N. Most nocturnal-type cloud clusters developed at this latitude (see Table 2). Maximum southerly winds occurred at 925 hPa near midnight (02 LST). A wind maximum with much smaller intensity shifted to 700 hPa at 14 LST. The atmosphere below 700 hPa was well mixed in the vertical, as indicated by the small vertical gradient in horizontal winds below 700 hPa.

Dynamic processes strengthening the LLJ are varied and complex. The effect of boundary-layer mixing on low-level wind can be explained by a simple dynamic analysis. Blackadar (1957) suggested clockwise veering in the ageostrophic low-level wind, as over the South Domain, could arise from an inertial oscillation in wind initiated by the sudden decoupling of strong turbulent mixing in the boundary layer after sunset. Trier and Parsons (1993) also suggested that a dramatic weakening of boundary-layer mixing in the evening could influence the nocturnal development, intensification, and pronounced veering of the LLJ. When the turbulent stress weakens as surface heating ceases, an inertial oscillation starts and the wind vector turns clockwise with time and intensifies. Such clockwise wind shifts were also apparent over the analysis domain, especially over the South Domain. The South Domain in this study is located around 30°N (25–32°N). Theoretical calculations show that an inertial oscillation has a period of one day at 30°N. The obvious diurnal variation in the low-level wind over the South Domain, could be an overlap in vertical variations driven by boundary-layer mixing, and horizontal variations driven by inertial oscillations with the same 1-day period. Wind oscillations are manifest in wind velocity changes. If no other force or motion (boundary-layer mixing and geostrophic motion) exists, horizontal winds will follow an inertial oscilla-

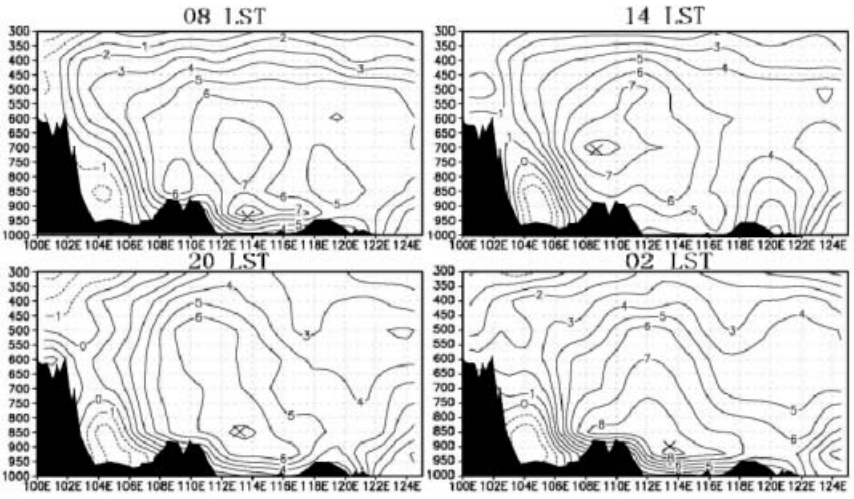

Fig. 21. Six-hourly (08, 14, 20, and 02 LST) longitude–height cross sections of v (m s^{-1}) averaged for 1–15 August 1998 at 30°N. A cross in each panel means the position of maximum v. Topography is shaded in the figure.

tion, a clockwise shift in wind direction with a period of 1 day.

Low-level moisture convergence in the MFCZ was due to nocturnal enhancement of the southwesterly S-LLJ south of the Meiyu front. The enhanced nocturnal LLJ, and the resultant low-level moisture convergence, increased convective instability (Fig. 16), synoptic-scale lifting, and low-level water vapor amounts in the MFCZ around midnight. Such factors can strengthen convection in the cloud cluster, resulting in enhancement of latent heat release in the cloud cluster.

Differences between the S-LLJ and the m-LLJ of clusters are not clear, especially near cloud clusters. It is also unclear whether the LLJ helps force the cloud cluster, or is a result of the cloud cluster. Many analyses have sought to demonstrate that the S-LLJ is independent from formation processes in cloud clusters within the Meiyu front (e.g., Chen and Yu 1988). Data in the present study show that a nocturnal, strong, low-level wind appeared every day from 1 to 15 August (Fig. 9), including periods when no cloud cluster developed. Similar analyses for June and July 1998 (not shown) confirm such independence of the S-LLJ from cloud cluster formation. Therefore, the diurnal cycle of the wind direction of the S-LLJ can enhance pre-existing cloud clusters but cannot generate cloud clusters.

8. Summary

This study used time series of GMS imagery to investigate the evolution of 61 long-lasting cloud clusters over eastern China that were observed during GAME/HUBEX IOPs in the 1998 and 1999 Meiyu seasons. More than two-thirds of the cloud clusters, named nocturnal-type clusters, attained a convective peak between midnight and early morning, with most peaking between 00 and 02 LST. Almost all of these nocturnal-type cloud clusters developed in, or south of the Meiyu frontal zone. The other clusters, named evening-type cloud clusters, peaked from late afternoon to evening, and were less intense than nocturnal-type clusters.

Moisture convergence over the MFCZ is key to the nocturnal development of cloud clusters. A weakening in boundary-layer mixing after sunset due to the cessation of solar radiation enhances the southwesterly S-LLJ over the South Domain. The stronger wind transports more water vapor after evening at low levels and forces a large moisture flux over the South Domain, causing a large area of low-level moisture convergence over the MFCZ. Enhanced moisture convergence increases the amount of water vapor, and the convective instability in the region.

Many studies have focused on the close relationship between the S-LLJ and rainfall sys-

tems along the Meiyu front. However, the nocturnal development of cloud clusters, and the contribution of the diurnal variation of the S-LLJ to cloud-cluster development, have seldom been studied. The present results show regulation in the evolution of cloud clusters along the Meiyu front and can assist in the forecasting of heavy rainfall associated with cloud-cluster convection peaks. Future work using data observed at finer spatial and temporal scales will clarify the dynamic processes controlling the interaction between the nocturnal development of cloud clusters, and the S-LLJ south of the Meiyu front.

Acknowledgements

We express deep gratitude to all of the Chinese and Japanese researchers who worked very hard during the GAME/HUBEX IOPs. We are grateful to Prof. K. Yamazaki, Prof. F. Hasebe, and Associate Prof. M. Watanabe of Hokkaido Univ. for their guidance and help. We would like to thank Mr. Y. Wakazuki and Mr. K. Arai for their technical support, Mr. Ohtake for his friendly encouragement during this study, Dr. H. Minda for offering the GMS data, and Dr. B. Geng for offering important information. We also acknowledge Prof. Y. Kodama (editor) and two anonymous reviewers for their helpful comments and their patience. The GAME-Reanalysis data derived from the advanced global forecasting model (T213L30) of the Japan Meteorology Agency and based on GAME/HUBEX observation data were used in this study. Figures presented in this work were made using GrADS software.

References

Akiyama, T., 1973: The large-scale aspects of the characteristic features of the Baiu Front. *Pap. Meteor. Geophys.*, **24**, 157–188.

Akiyama, T., 1984a: A medium-scale cloud cluster in a Baiu front. Part I. Evolution process and fine structure. *J. Meteor. Soc. Japan*, **62**, 485–504.

Akiyama, T., 1984b: A medium-scale cloud cluster in a Baiu front. Part II. Thermal and kinematic fields and heat budgets. *J. Meteor. Soc. Japan*, **62**, 505–521.

Anderson, C.J. and R.W. Arritt, 1998: Mesoscale convective complexes and persistent elongated convective systems over the United States during 1992 and 1993. *Mon. Wea. Rev.*, **126**, 578–599.

Asai, T., S. Ke, and Y. Kodama, 1998: Diurnal variability of cloudiness over East Asia and the western Pacific Ocean as revealed by GMS during the warm season. *J. Meteor. Soc. Japan*, **76**, 675–684.

Blackadar, A.K., 1957: Boundary-layer wind maxima and their significance for the growth of nocturnal inversions. *Bull. Amer. Meteor. Soc.*, **38**, 283–290.

Chen, G.T.-J., 1983: Observational aspects of the Mei-yu phenomenon in subtropical China. *J. Meteor. Soc. Japan*, **61**, 306–312.

Chen, G.T.-J. and C.-C. Yu, 1988: Study of low-level jet and extremely heavy rainfall over northern Taiwan in the Mei-yu season. *Mon. Wea. Rev.*, **116**, 884–891.

Chen, C., W.-K. Tao, P.-L. Lin, G.S. Lai, S.-F. Tseng, and T.-C.C. Wang, 1998a: The intensification of the low-level jet during the development of mesoscale convective systems on a Mei-yu front. *Mon. Wea. Rev.*, **126**, 349–371.

Chen, S.-J., Y.-H. Kao, W. Wang, Z.-Y. Tao, and B. Cui, 1998b: A modeling case study of heavy rainstorms along the Mei-yu front. *Mon. Wea. Rev.*, **126**, 2330–2351.

Cotton, W.R., R.L. George, P.J. Wetzel, and R.L. McAnelly, 1983: A long-lasting mesoscale convective complex. Part I: The mountain-generated component. *Mon. Wea. Rev.*, **111**, 1893–1918.

Ding, Y.-H., 1992: Summer monsoon rainfalls in China. *J. Meteor. Soc. Japan*, **70**, 373–396.

Ding, Y.-H. and Y. Liu, 2000: The relationship between the activities of the summer monsoon and severe flooding in China in 1998. Proc. International Conference on Mesoscale Convective Systems and Heavy Rainfall in East Asia, Soul, Korea, 45–66.

Ding, Y.-H., Y. Zhang, Q. Ma, and G. Hu, 2001: Analysis of the large-scale circulation features and synoptic systems in east Asia during the intensive observation period of GAME/HUBEX. *J. Meteor. Soc. Japan*, **79** (1B), 277–300.

Fujiyoshi, Y., Y.-H. Ding, and Y. Zhang, 2006: Outline of GAME/HUBEX, Final report of GAME/HUBEX (ed. Y. Fujiyoshi and Y.-H. Ding), *GAME Publication* No. **43**, 1–6.

Gray, W.M. and R.W. Jacobson, Jr., 1977: Diurnal variation of deep cumulus convection. *Mon. Wea. Rev.*, **105**, 1171–1187.

Iwasaki, H. and T. Takeda, 1993: Structure and behavior of mesoscale cloud clusters traveling over the Baiu-frontal zone. *J. Meteor. Soc. Japan*, **71**, 733–747.

Kato, K., 1985: On the abrupt change in the structure of the Baiu front over the China continent in late May of 1979. *J. Meteor. Soc. Japan*, **63**, 20–36.

Kato, K., J. Matsumoto, and H. Iwasaki, 1995: Diurnal variation of Cb-clusters over China and its relation to Large-scale conditions in the summer of 1979. *J. Meteor. Soc. Japan*, **73**, 1219–1234.

Kubota, H. and T. Nitta, 2001: Diurnal variations of tropical convection observed during the TOGA-COARE. *J. Meteor. Soc. Japan*, **79**, 815–830.

Leary, C.A. and E.N. Rappaport, 1987: The life cycle and internal structure of a mesoscale convective complex. *Mon. Wea. Rev.*, **115**, 1503–1527.

Maddox, R.A., 1980: Mesoscale convective complexes. *Bull. Amer. Meteor. Soc.*, **61**, 1374–1387.

Maddox, R.A., 1983: Large-scale meteorological conditions associated with midlatitude, mesoscale convective complexes. *Mon. Wea. Rev.*, **111**, 1475–1493.

Mapes, B.E. and R.A. Houze, Jr., 1993: Cloud clusters and superclusters over the oceanic warm pool. *Mon. Wea. Rev.*, **121**, 1398–1415.

Matsumoto, S., S. Yoshizumi, and M. Takeuchi, 1970: On the structure of the Baiu front and the associated inter mediate-scale disturbances in the lower atmosphere. *J. Meteor. Soc. Japan*, **48**, 479–491.

Misumi, Y., 1999: Diurnal variations of precipitation grouped into cloud categories around the Japanese archipelago in the warm season. *J. Meteor. Soc. Japan*, **77**, 615–635.

Ninomiya, K. and T. Akiyama, 1971: The development of the medium-scale disturbance in the Baiu front. *J. Meteor. Soc. Japan*, **49**, 663–677.

Ninomiya, K. and T. Akiyama, 1974: Band structure of mesoscale echo clusters associated with low-level jet stream. *J. Meteor. Soc. Japan*, **52**, 300–313.

Ninomiya, K., M. Ikawa, and T. Akiyama, 1981: Long-lasting medium-scale cumulonimbus cluster in Asian subtropical humid region. *J. Meteor. Soc. Japan*, **59**, 564–577.

Ninomiya, K., T. Akiyama, and M. Ikawa, 1988a: Evolution and fine structure of a long-lasting meso-α-scale convective system in Baiu frontal zone. Part I: Evolution and meso-β-scale characteristics. *J. Meteor. Soc. Japan*, **66**, 331–350.

Ninomiya, K., T. Akiyama, and M. Ikawa, 1988b: Evolution and fine structure of a long-lasting meso-α-scale convective system in Baiu frontal zone. Part II: Meso-γ-scale characteristics of precipitation. *J. Meteor. Soc. Japan*, **66**, 351–370.

Ninomiya, K. and Y. Tatsumi, 1981: Forecast experiment of long-lasting subtropical cumulonimbus cluster with 6-level 77 km-mesh primitive model. *J. Meteor. Soc. Japan*, **59**, 709–722.

Ohsawa, T., H. Ueda, T. Hayashi, A. Watanabe, and J. Matsumoto, 2001: Diurnal variations of convective activity and rainfall in tropical Asia. *J. Meteor. Soc. Japan*, **79**, 333–352.

Randall, D., A. Harshvardan, and D.A. Dazlich, 1991: Diurnal variability of the hydrologic cycle in a general circulation model. *J. Atmos. Sci.*, **48**, 40–62.

Shinoda, T. and H. Uyeda, 2002: Effective factors in the development of deep convective clouds over the wet region of Eastern China during the summer monsoon season. *J. Meteor. Soc. Japan*, **80**, 1395–1414.

Sui, C.H., K.M. Lau, Y.N. Takayabu, and d.A. Short, 1997: Dirunal variations in tropical oceanic cumulus convection during TOGA COARE. *J. Atmos. Sci.*, **54**, 639–655.

Takeda, T. and H. Iwasaki, 1987: Some characteristics of meso-scale cloud clusters observed in East Asia between March and October 1980. *J. Meteor. Soc. Japan*, **65**, 507–513.

Tao, S.-Y., Y.-H. Ding, S.-Q. Sun, A.-Y. Cai, M.-D. Zhang, Z.-Y. Fang, M.-T. Li, X.-P. Zhou, S.-X. Zhao, S.-T. Dian, Y.-L. Li, Q.-J. Zhu, and Q.-Y. Zhang, 1980: *Severe rainstorms in China*. Science Press, 225 pp.

Trier, S.B. and D.B. Parsons, 1993: Evolution of environmental conditions preceding the development of a nocturnal mesoscale convective complex. *Mon. Wea. Rev.*, **121**, 1078–1098.

Wetzel, P.J., W.R. Cotton, and R.L. McAnelly, 1983: A long-lasting mesoscale convective complex. Part II: Evolution and structure of the mature complex. *Mon. Wea. Rev.*, **111**, 1919–1937.